Photonics and Nanostructures - Fundamentals and Applications 32 (2018) 6–10

Contents lists available at ScienceDirect

Photonics and Nanostructures - Fundamentals and Applications

journal homepage: www.elsevier.com/locate/photonics

Transmission spectra of one-dimensional porous alumina photonic crystals

V.S. Gorelik[a,b], P.P. Sverbil[a,*], V.V. Filatov[a,b], Dongxue Bi[a,b], Guang Tao Fei[c], Shao Hui Xu[c]

[a] Lebedev Physical Institute of the Russian Academy of Sciences, Moscow, 119991, Russia
[b] Bauman Moscow State Technical University, Moscow, 105005, Russia
[c] Key Laboratory of Materials Physics and Anhui Key Laboratory of Nanomaterials and Nanotechnology, Institute of Solid State Physics, Hefei Institutes of Physical Science, Chinese Academy of Sciences, Hefei, 230031, China

ARTICLE INFO

Keywords:
Photonic crystal
Porous alumina
Stop band
Narrow-band filter
Raman scattering enhancement
Sensor

ABSTRACT

The optical properties of a one-dimensional photonic crystal based on porous alumina with a crystal lattice constant of 460 nm were studied. The experimentally measured transmission spectrum of a one-dimensional photonic crystal film was compared with the theoretical spectrum in the spectral regions corresponding to the first, second, and third stop bands. The potential for using one-dimensional porous alumina photonic crystals as selective narrow-band filters and sensors was analyzed. Embedding a Raman-active medium into the voids of porous photonic crystal should provide an essential increase of spontaneous Raman scattering signal and low-threshold stimulated Raman scattering. The amount of substance needed for recording Raman spectra may be substantially decreased.

1. Introduction

At present, it is very important to create new types of optical filters and sensors with controlled optical properties. In this connection, it is of great interest to study photonic crystal (PhC) [1–4] media with spatial variation of dielectric permittivity. One type of PhCs is the one-dimensional (1D) PhC constructed from alternating layers with two different refractive indices. In the reflection spectrum of such crystal, there are spectral regions where strong reflection of electromagnetic radiation from the surface of the crystal is observed. Such areas are referred to as photonic bandgaps, or stop bands. The spectral positions of the stop bands depend on the parameters of the PhC, i.e., the crystal lattice constant and the values of the refractive indices. PhCs are used in various applications [5–9].

One of the kinds of PhCs is a porous structure containing pores with a size of tens of nanometers [4,10,11]. The optical properties of a porous globular PhC constructed of close-packed silica globules (SiO_2) in the form of a face-centered cubic lattice have been previously studied [12–15]. In recent years, a method for producing porous 1D PhCs by the electrochemical etching of silicon and aluminum has been developed [11,16–20]. As a result, PhC films of porous alumina (PA) were produced. The lattice constant of these PhCs depends on the etching regime and can vary within the range of 100–500 nm. The aim of this paper is to investigate the optical properties of 1D PhC films based on PA with different pore fillings in order to control their transmission and Raman spectra.

2. Experimental procedure and experimental results

A thin multilayered film (20 μm) of PA fabricated by the anodization of a given area of the surface of aluminum plate was used as the sample for the study. In the anodization process, a periodic current was passed (Fig. 1) through the aluminum plate in an acidic solution. Pulse durations were approximately 200 s for the maximum current with the period of approximately 15 min. As a result, a periodical PA structure (1D PA PhC) was formed. This structure consists of dielectric layers of two kinds with different porosities and different average refractive indices, as shown schematically in Fig. 2.

At the center of the sample, there is a PA PhC film with a thickness of approximately 20 μm. This film is surrounded by an un-etched portion of an aluminum plate with a thickness of approximately 300 μm, which serves as a holder for a PA PhC. SEM images of the surface (a) and the slice (b) of the PA PhC film are shown in Fig. 3. The inset in this figure presents the photograph of the sample. The pores of the PA have a size of 80–85 nm (see Fig. 3a), and the lattice constant of PhC is $d = 460 \pm 10$ nm (see Fig. 3b).

We recorded the transmission spectrum of the PA PhC with radiation from a xenon lamp. Fig. 4 shows the measured transmission spectrum $T(\lambda)$ of the PA PhC under study in the wavelength range of 300–2000 nm at zero incidence angle.

* Corresponding author.
E-mail address: sverbil@sci.lebedev.ru (P.P. Sverbil).

https://doi.org/10.1016/j.photonics.2018.08.004
Received 16 December 2017; Received in revised form 10 August 2018; Accepted 27 August 2018
Available online 30 August 2018

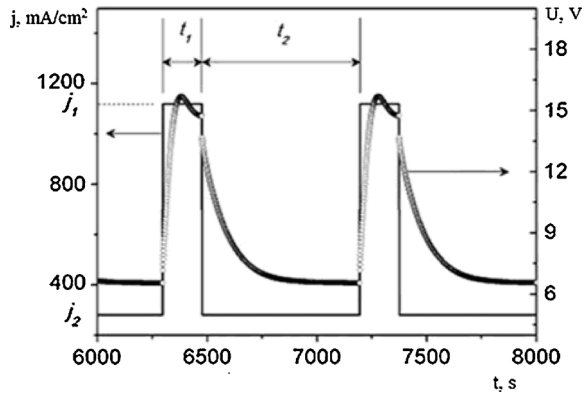

Fig. 1. Typical current-time dependence during the formation of the periodical PA structure.

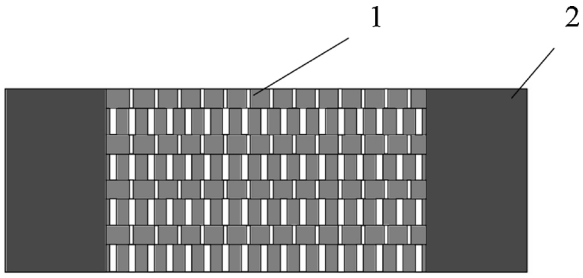

Fig. 2. Structure of the investigated sample: 1 –multilayered PA film, 2 – aluminum holder.

From Fig. 4, it can be seen that the transmittance of this PA PhC exhibits sharp minima in the regions corresponding to the first, second, and third stop bands located at wavelengths of approximately 1260, 630, and 420 nm, respectively.

3. Discussion of experimental results

Fig. 3a shows that the film under study has pores much smaller than the wavelengths of incident radiation during transmission measurement. These pores form a two-dimensional (2D) quasi-hexagonal lattice with an average distance between pores of 150–200 nm. When considering the scattering of a plane electromagnetic wave by such 2D structure, it is necessary to consider the formation of plane waves of different diffraction orders [21,22]. Our estimation gives a possible wavelength range of 200–300 nm and shorter for the 90° diffraction inside the PA layer and 150–200 nm range and shorter for the diffraction outside the layer. These effects may be responsible for lowering the transmission at short wavelengths. Thus, diffraction effects are not essential in the visible and infrared ranges. Therefore, because the wavelength range of 300–2000 nm is studied in this paper, we shall neglect diffraction and consider each layer of this multilayer structure as a homogeneous medium with the corresponding refractive index n_j. Such a film can be considered as a 1D PhC. The dispersion law for the PhC was proposed on the basis of the 1D PhC model given in [23]. In this model, a periodical structure of homogeneous dielectric layers of two kinds is considered. The dispersion law of electromagnetic waves in a 1D PhC with an infinite number of layers is given by the following expression:

$$\cos kd = \cos k_1 a_1 \times \cos k_2 a_2 - \frac{1}{2}\left(\frac{n_1}{n_2} + \frac{n_2}{n_1}\right)\sin k_1 a_1 \times \sin k_2 a_2. \quad (1)$$

Here, n_1 and n_2 are the refractive indices of the composite layers with thicknesses of a_1 and a_2, respectively; $k_1 = \frac{\omega}{c}\cdot n_1$, $k_2 = \frac{\omega}{c}\cdot n_2$; ω is the cycle frequency and k is the wave vector of an electromagnetic wave; $c = 3 \times 10^8$ m/s is the speed of light in vacuum; and $d = a_1 + a_2$ is the lattice constant of the PhC. We assume all the media to be non-magnetic ($\mu = 1$). The corresponding dispersion curve $\omega(k)$ derived from (1) is shown in Fig. 5. There are regions of stop bands at $k = 0$ (for the second dispersion branch) and $k = k_{max}$.

The spectral positions of the stop bands of a PhC obey the well-known Wulff-Bragg's law:

$$m\cdot\lambda_m = 2d\cdot\sqrt{n_{ef}^2 - \sin^2\theta}\,. \quad (2)$$

Here $m = 1,2,3$ are the numbers of the corresponding stop bands; λ_m is the wavelength corresponding to a certain stop band; and θ is the angle of incidence of light on the PhC. The value of n_{ef} is calculated from the relation

$$n_{ef}^2 = \frac{a_1}{a_1 + a_2}n_1^2 + \frac{a_2}{a_1 + a_2}n_2^2, \quad (3)$$

where n_1 and n_2 are the refractive indices of the corresponding layers.

The width of the stop band with the ordinal number m is connected with the refractive indices of the layers by the following relation [23]:

$$\frac{\Delta\lambda}{\lambda} = \frac{4}{\pi\cdot m}\cdot\frac{|n_1 - n_2|}{n_1 + n_2}. \quad (4)$$

Several methods of analyzing the optical properties of a finite 1D PhC were described in [24–31]. We have calculated the transmission spectra using the transfer matrix method (TMM – [24], Section 1.6). In each region of a multilayered 1D structure, the electric field e_j can be written as follows:

$$e_j = t_j exp(ik_j x) + r_j exp(-ik_j x), \quad (5)$$

where t_j and r_j are the amplitudes of the waves propagating in the incident light direction and in the opposite direction, respectively. In the general case, if the layers are numbered from left to right, and the light is incident from the left, these amplitudes in adjacent layers fit the following relation:

$$(t_j, r_j) = \mathbf{M}_j(t_{j-1}, r_{j-1}), \quad (6)$$

where t_j and r_j are the wave amplitudes after the j-th layer, t_{j-1} and r_{j-1} are the wave amplitudes before the j-th layer, and $\mathbf{M}_j$ is the so-called transfer matrix of the j-th layer. In the case of a homogeneous layer with a refractive index n_j and thickness a_j, the coefficients of such 2×2 matrix can be written in the form

$$\mathrm{M}_j = \begin{bmatrix} \cos(k_0 n_j a_j) & -\frac{i}{n}\sin(k_0 n_j a_j) \\ -i\cdot n\cdot\sin(k_0 n_j a_j) & \cos(k_0 n_j a_j) \end{bmatrix}, \quad (7)$$

where k_0 is the wave vector of the incident light in vacuum ($k_0 = 2\pi/\lambda$); all media are assumed to be non-magnetic ($\mu = 1$), and the angle between the wave vector and the X-axis of the structure is assumed to be zero.

To derive the wave amplitudes for a structure composed of j layers, one can successively apply the following matrix relation (6):

$$(t_j, r_j) = \mathbf{M}_j{*}\mathbf{M}_{j-1}{*}\ldots{*}\mathbf{M}_1(t_0, r_0). \quad (8)$$

If we consider a periodical 1-2-1-2-…1-2 structure with an even number of layers $j = 2s$, so that $\mathbf{M}_1 = \mathbf{M}_3 = \ldots = \mathbf{M}_{2s-1}$ and $\mathbf{M}_2 = \mathbf{M}_4 = \ldots = \mathbf{M}_{2s}$, then

$$(t_j, r_j) = (\mathbf{M}_2{*}\mathrm{M}_1)^s(t_0, r_0) = \mathbf{M}\,(t_0, r_0), \quad (9)$$

$$(t_0, r_0) = \mathbf{M}^{-1}\,(t_j, r_j), \quad (10)$$

where $\mathbf{M}$ is the transfer matrix of the whole structure and $\mathbf{M}^{-1}$ is the inverse transfer matrix.

Starting with $t_j = 1$, $r_j = 0$ (corresponding to the waves that have passed through the layered structure from the left to the right half-space, where only the transmitted component exists) from (10), one can find the amplitudes t_0, r_0 of the waves incident on and reflected from the structure in the left half-space. Then, the amplitude transmission of

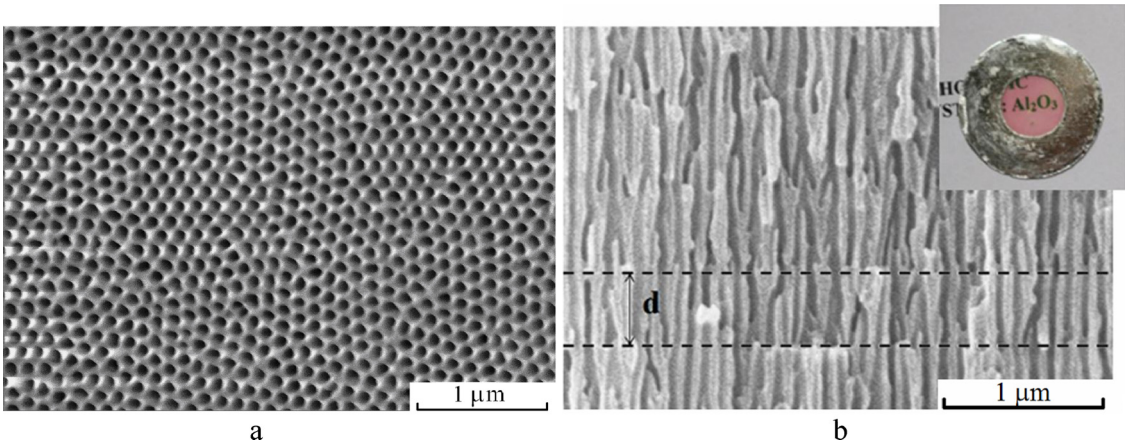

Fig. 3. SEM images of surface (a) and slice (b) of one-dimensional PhC based on PA; lattice constant of PhC is d = 460 ± 10 nm. A photograph of investigated sample is shown in the inset.

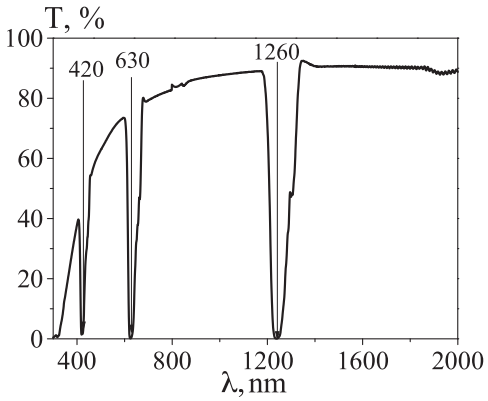

Fig. 4. A transmission spectrum of the PA PhC sample.

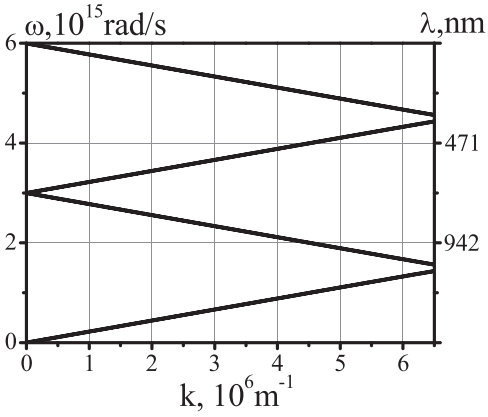

Fig. 5. Dispersion curves *ω(k)* for electromagnetic waves propagating in 1D PhC.

the multilayered structure $t = t_j/t_0$ and intensity transmission T(λ) can be calculated for each given λ as follows:

$$T = \left|\frac{t_j}{t_0}\right|^2 \tag{11}$$

In our case, we approximated PA PhC by a periodical structure comprising two homogeneous layers with thicknesses a_1 and a_2 and refractive indices n_1 and n_2, respectively. We assume that the lattice constant of the PhC is $d = a_1 + a_2 = 460$ nm (Fig. 3), the number of layers j = 88. From relation (2) and the position of the first stop band ($\lambda_1 = 1260$ nm) in Fig. 4, we derived the value of the effective refractive index of the PhC $n_{ef} = 1.37$. Considering relations (3) and (4) and the spectral width ($\Delta\lambda = 80$ nm) of the first stop band (see Fig. 4), we derived the values of the refractive indices n_1 and n_2 of the layers to be $n_1 = 1.43$ and $n_2 = 1.30$. These parameters were used in relations (6–11) for calculating the transmission spectra by the TMM. We started from $a_1 = a_2 = 230$ nm, and the best fit with experimental spectrum was obtained at $a_1 = 260$ nm and $a_2 = 200$ nm.

The experimental (solid line) and theoretical (dashed line) transmission spectra of the investigated sample are shown in Fig. 6. As can be seen from this figure, the recorded transmission spectrum (solid line in Fig. 6) is close to the calculated one (dashed line). Visible oscillations appearing on the theoretical curve are due to the interference of the waves reflected from different layers. The observed differences between the recorded and calculated values result from slight variations of the thickness and refractive index of the layers in the analyzed PhC film. These variations may be responsible for the damping of fast oscillations in the registered transmission curve.

We propose a narrow-band filter based on a filled PhC, which provides selective reflection of laser radiation at a given wavelength. The required change in the characteristics of a porous 1D PhC can be achieved by introducing other substances into the voids of such crystal. In this case, the effective refractive index is varied. In accordance with the Wulff-Bragg's law (2), this leads to a change in the spectral position of the stop bands and their spectral widths. For example, lithium iodate ($LiIO_3$) may be introduced into the voids of the PA. This substance is highly soluble in water. Thus, it is possible to fill the PA PhC with the corresponding aqueous solution and then evaporate the liquid.

The refractive index of lithium iodate is $n_f = 1.90$. Filling PA with

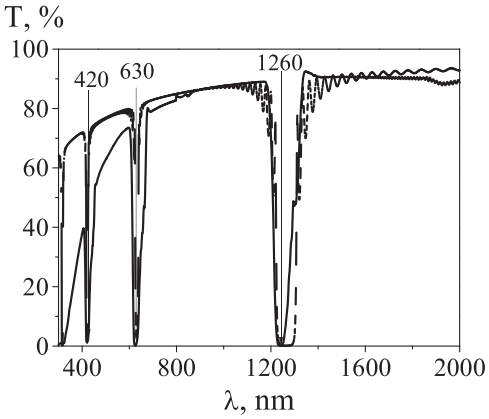

Fig. 6. Comparison between experimental (solid line) and theoretical (dashed line) transmission spectra of investigated PA PhC.

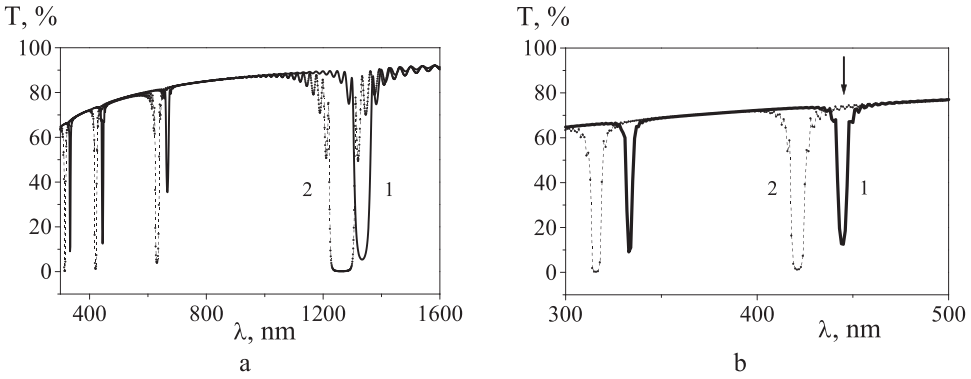

Fig. 7. Transmission spectra of 1D PA PhC filled with $LiIO_3$ (η = 0.24, curves 1) and without filling (η = 0, curves 2) at 300–1600 nm (a) and 300–500 nm (b) spectral ranges. The arrow in Fig. 7b indicates the position of the laser line to be filtered (λ_m = 445 nm).

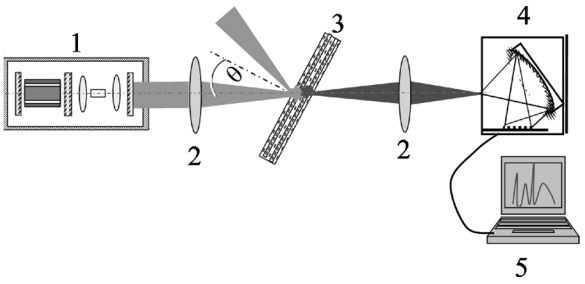

Fig. 8. Schematic diagram of experimental setup for observing low-threshold stimulated Raman scattering; 1-YAG:Nd^{3+} laser (operating at 0.532 μm), 2-lenses, 3-PhC filled with Raman active media, 4-minispectrometer, 5-computer.

lithium iodate provides the following value of the refractive index of each layer:

$$n_j = \sqrt{(1-\delta_j)\cdot n_s^2 + \delta_j\cdot(1-\eta)\cdot n_0^2 + \delta_j\cdot\eta\cdot n_f^2}\,. \quad (12)$$

Here, δ_j (j = 1,2) is the porosity of PA (its value depends on etching conditions), n_s = 1.76 is the refractive index of bulk alumina, n_0 = 1 is the refractive index of the air, and

η is the factor of PA filling with $LiIO_3$. The filling factors required for the film under study are η = 0.02 for the second stop band to match λ_m = 633 nm and η = 0.24 for the third stop band to match λ_m = 445 nm. The shift of the transmission curve of the 1D PA PhC at η = 0.24 needed for filtering the laser line of 445 nm is illustrated in Fig. 7(a,b). In addition, the fine tuning of the reflection band of a PhC is

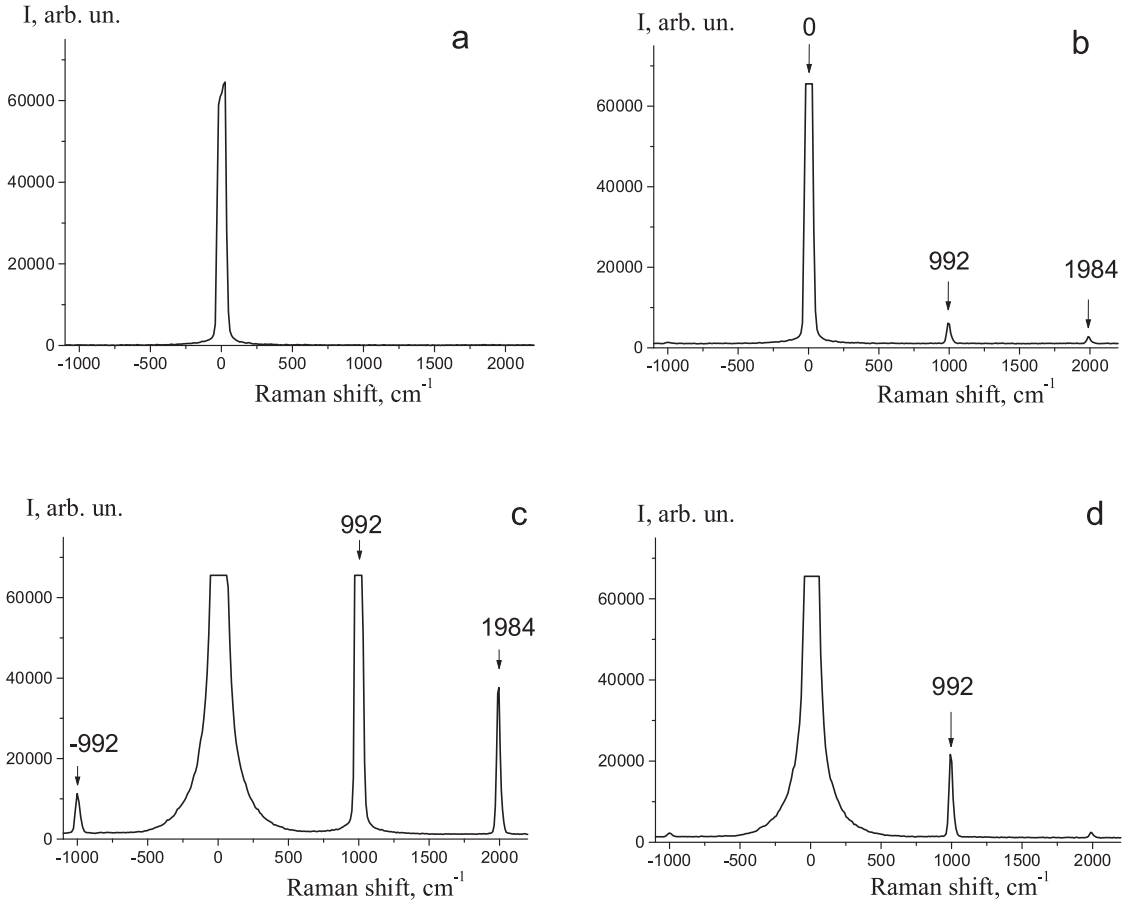

Fig. 9. Spectra of SRS in porous PhC filled with benzene excited by 532 nm YAG:Nd^{3+} pulsed laser at angles of incidence of 20° (a), 30° (b), 40° (c), and 50° (d). The pump intensity was 0.12 GW/cm^2.

achieved when it is rotated by a certain angle θ in accordance with the Wulff-Bragg's law.

The experiments with porous PhCs infiltrated by molecular liquids indicate that the threshold of stimulated Raman scattering in porous PhC is significantly lower than that in homogeneous Raman-active materials when the frequency of pump radiation fits the spectral region of the stop band (the experimental setup is shown in Fig. 8). The group velocity of exciting light waves inside the PhC decreases to very low values at a certain angle θ, according to (2), when the frequency of the exciting light is close to the edge of the photonic band gap. This, in turn, leads to a sharp increase in the photonic density of states and remarkable enhancement of spontaneous Raman scattering cross-section for the substance embedded into the voids of porous PhC.

We have observed such a sharp increase in the Raman intensity in PhCs filled with benzene and carbon disulfide [32] at certain angles of incidence. When the pores of a PhC were filled with an active medium for stimulated Raman scattering (SRS), low-threshold SRS was observed. SRS was excited by the second optical harmonics (532 nm, 7 mJ in each laser pulse with a 10 ns duration and 10 Hz repetition rate) of YAG: Nd^{3+} laser, collimated on the sample by the lens. SRS radiation was registered in a wide range by the "Ocean Optics" minispectrometer. SRS spectra in PhC filled with benzene registered at various angles of incidence are presented in Fig. 9 (the pump intensity was 0.12 GW/cm^2).

The first Stokes component in SRS spectra appeared at 0.09 GW/cm^2 in PhC with benzene and 0.07 GW/cm^2 in PhC with carbon disulfide. For comparison, when carbon disulfide was used as the active medium at a pump intensity of 70 MW/cm^2, the first Stokes component of stimulated Raman forward scattering appeared in a spectrum of the radiation that passed a 10 cm long cuvette. The SRS gain raised by more than an order of magnitude at a certain angle θ of the PhC (40° for benzene and 60° for carbon disulfide), and additional Stokes and anti-Stokes Raman satellites appeared in the spectrum. This is explained by the large increase in the photonic density of states in the case when the frequency of the exciting light or SRS radiation is close to the edge of the corresponding stop band [28].

4. Conclusion

Thus, the transmission spectrum of the 1D PA PhCs with a lattice constant of d = 460 nm produced by the electrochemical etching of an aluminum plate was studied. The spectral positions of the first three stop bands of this PA PhC were determined. The experimental and theoretical data obtained for the transmission spectra were compared. A satisfactory agreement between theory and experiment was demonstrated. Changes in the PhC parameters (the lattice constant and the amount of substance introduced into the pores of the PhC) affect the spectral position and width of the stop bands. By using the investigated PA PhC, narrow-band filters promising for the recording of Raman spectra can be developed. In this case, the fine tuning of the reflection band of a PhC is achieved when it is rotated by a certain angle θ in accordance with the Wulff-Bragg's law. Embedding a Raman-active medium into the voids of the discussed porous PhC should provide an essential increase of spontaneous Raman scattering signal and low-threshold stimulated Raman scattering, and the amount of substance needed for recording Raman spectra may be substantially decreased. Thus, PA PhCs filled with Raman-active medium may be used as effective molecular compound sensors.

Acknowledgments

This work was partially supported by the Russian Foundation for Basic Research (grant 18-02-00181-a), the National Natural Science Foundation of China (grant 51671183) and the China Scholarship Council.

References

[1] V.P. Bykov, Spontaneous emission in a periodic structure, Sov. J. Exp. Theor. Phys. 35 (1972) 269–273.
[2] E. Yablonovitch, Inhibited spontaneous emission in solid-state physics and electronics, Phys. Rev. Lett. 58 (1987) 2059–2062.
[3] S. John, Strong localization of photons in certain disordered dielectric superlattices, Phys. Rev. Lett. 58 (1987) 2486–2489.
[4] V.S. Gorelik, Optics of globular photonic crystals, Quant. Elec. 37 (2007) 409–432.
[5] K. Asakawa, Y. Sugimoto, Y. Watanabe, N. Ozaki, A. Mizutani, Y. Takata, Y. Kitagawa, H. Ishikawa, N. Ikeda, K. Awazu, X. Wang, A. Watanabe, S. Nakamura, S. Ohkouchi, K. Inoue, M. Kristensen, O. Sigmund, P.I. Bore, R. Baets, Photonic crystal and quantum dot technologies for all-optical switch and logic device, New J. Phys. 8 (2006) 208.
[6] V.S. Gorelik, Linear and nonlinear optical phenomena in nanostructured photonic crystals, filled by dielectrics or metals, Eur. Phys. J. Appl. Phys. 49 (2010) 33007.
[7] P. Lodahl, A.F. van Driel, I.S. Nikolaev, A. Irman, K. Overgaag, D. Vanmaekelbergh, W.L. Vos, Controlling the dynamics of spontaneous emission from quantum dots by photonic crystals, Nature 430 (2004) 654–657.
[8] C.H.R. Ooi, T.C. Au Yeung, C.H. Kam, T.K. Lim, Photonic band gap in a superconductor-dielectric superlattice, Phys. Rev. B 61 (2000) 5920–5923.
[9] C.-J. Wu, M.-S. Chen, T.-J. Yang, Photonic band structure for a superconductor-dielectric superlattice, Phys. C Supercond. 432 (2005) 133–139.
[10] Liu Yisen, Chang Yi, Ling Zhiyuan, Hu Xing, Li Yi, Structural coloring of aluminum, Electrochem. commun. 13 (2011) 1336–1339.
[11] S.E. Svyakhovskiy, A.I. Maydykovsky, T.V. Murzina, Mesoporous silicon photonic structures with thousands of periods, J. Appl. Phys. 112 (2012) 013106.
[12] E.L. Ivchenko, A.N. Poddubny, Resonant three-dimensional photonic crystals, Phys. Solid State 48 (2006) 581–588.
[13] V.V. Filatov, V.S. Gorelik, Dispersion relation of acoustic waves in phononic crystals filled with dielectric or metal, Bull. Lebedev Phys. Inst. 37 (2010) 56–57.
[14] V.S. Gorelik, V.V. Filatov, Dispersion characteristics of water- and gold-infiltrated opal photonic crystals, Inorg. Mater. 48 (2012) 361–367.
[15] V.S. Gorelik, L.S. Lepnev, A.O. Litvinova, Conversion of short-wavelength electromagnetic radiation in SiO_2 opal photonic crystals, Inorg. Mater. 50 (2014) 1003–1006.
[16] L. Pavesi, Porous silicon dielectric multilayers and microcavities, La Riv. Del Nuovo Cimento Ser. 3 20 (1997) 1–76.
[17] U. Grüning, V. Lehmann, C.M. Engelhardt, Two-dimensional infrared photonic band gap structure based on porous silicon, Appl. Phys. Lett. 66 (1995) 3254–3256.
[18] H. Masuda, M. Ohya, H. Asoh, M. Nakao, M. Nohtomi, T. Tamamura, Photonic crystal using anodic porous alumina, Japanese J. Appl. Phys. 38 (1999) L1403–L1405.
[19] B. Wang, G.T. Fei, M. Wang, M.G. Kong, L.D. Zhang, Preparation of photonic crystals made of air pores in anodic alumina, Nanotechnology 18 (2007) 365601.
[20] A. Santos, Nanoporous anodic alumina photonic crystals: fundamentals, developments and perspectives, J. Mater. Chem. C 5 (2017) 5581–5599.
[21] M.V. Rybin, K.B. Samusev, S. Yu, Yu.S. Lukashenko, M.F. Kivshar, Limonov, Transition from two-dimensional photonic crystals to dielectric metasurfaces in the optical diffraction with a fine structure, Sci. Rep. 6 (2017) 30773.
[22] M.V. Rybin, I.S. Sinev, A.K. Samusev, K.B. Samusev, E. Yu, D.A. Trofimova, V.G. Kurdyukov, M.F. Golubev, Limonov, Dimensionality effects on the optical diffraction from opal-based photonic structures, Phys. Rev. B 87 (2013) 125131.
[23] A. Yariv, P. Yeh, Optical Waves in Crystals, Wiley, N.Y, 1984.
[24] M. Born, E. Wolf, Principles of Optics, 4th.ed., Pergamon Press, Oxford, 1970.
[25] H.A. Gómez-Urreaa, C.A. Duquea, M.E. Mora-Ramos, Bulk-like-phonon polaritons in one-dimensional photonic superlattices, Photon. Nanostruct. 24 (2017) 7–11.
[26] Y. Iqbal, M. Faryad, Photonic band structures of one dimensional multilayered dielectric-magnetic photonic crystals, Photon. Nanostruct. 24 (2017) 63–68.
[27] V.S. Gorelik, Optics of globular photonic crystals, Laser Phys. 18 (2008) 1479–1500.
[28] V.S. Gorelik, V.V. Kapaev, Electromagnetic-field amplification in finite one-dimensional photonic crystals, J. Exp. Theor. Phys. 123 (2016) 373–381.
[29] V.S. Gorelik, S.O. Klimonskii, V.V. Filatov, K.S. Napol'skii, Optical properties of one-dimensional photonic crystals based on porous films of anodic aluminum oxide, Opt. Spectrosc. 120 (2016) 534–539.
[30] V.S. Gorelik, A.V. Pudovkin, V.V. Filatov, Mesoporous photonic-crystal films for amplification and filtering of electromagnetic radiation, J. Russ. Laser Res. 37 (2016) 604–610.
[31] V.S. Gorelik, M.M. Yashin, A.I. Vodchits, Reflection spectra of 1D photonic crystals based on aluminum oxide, Phys. Wave Phenom. 25 (2017) 175–179.
[32] Y. Almohamed, R. Barille, A.I. Vodchits, Yu.P. Voinov, V.S. Gorelik, A.D. Kudryavtseva, V.A. Orlovich, N.V. Chernega, Reduction of the threshold of stimulated raman scattering in raman-active media introduced into pores of a globular photonic crystal, JETP Lett. 101 (2015) 365–370.